1. Aly MM, Saitoh Y, Hosomi K, Oshino S, Kishima H, Yoshimine T. Spinal cord stimulation for central poststroke pain. *Neurosurgery*. 2010;67(3): ONS206-ONS212.
2. Lopez JA, Torres LM, Gala F, Iglesias I. Spinal cord stimulation and thalamic pain: long term results of eight cases. *Neuromodulation*. 2009;12(3): 240-243.
3. Stojanovic M, Abdi S. Spinal cord stimulation. *Pain Phys*. 2002;5(2):156-166.
4. Coffey RJ, Lozano AM. Neurostimulation for chronic noncancer pain: an evaluation of the clinical evidence and recommendations for future trial designs. *J Neurosurg*. 2006;105(2):175-198.

10.1227/NEU.0b013e318210f04b

## Neurosurgery Simulation

In their neurosurgery simulation technology review, Malone et al[1] address an important yet largely unaddressed surgical area that can significantly benefit from the availability of an effective simulation-based surgical training system. Further, they touch on a number of relevant aspects of developments that will underpin their work on a pedicle screw placement simulator. We would like to add some additional thoughts here, which are based our work over the past several years in developing both a hard-tissue (burr hole) drilling simulator prototype for the US Army as well as a generalized soft-tissue simulation and bleeding system for general surgical resident training.

The authors have correctly identified that the foundational step in developing a system that provides clinically useful surgical skills training is to isolate the subtasks that will benefit most from simulation. Minimizing effort devoted to already mastered or commonly acquired skills and, instead, focusing on critical skill areas that are not well addressed with currently available approaches is critical to producing a simulator that meets unmet needs. To build simulations for those subtasks, the movements and loads experienced by the surgeon during both expected and unexpected actions in the procedure need to form the basis for the mathematical modeling and haptic device interfaces that will be developed. We have also found that, as the authors note, these movements and loads are often not known/available, and we have had to obtain this information ourselves as well. Measuring how actions are done wrong is just as important, if not more so, as measuring when they are done correctly, because an effective simulator must provide learners with the complete range of possible interactions. Learning what happens when something is done right often occurs in the context of learning what happens when things are done wrong.

Also important at the earliest stage of planning a simulator is defining objective, quantitative metrics of performance that can be used to measure attainment of proficiency of the skills being learned. This enables the simulator to be designed to provide reliable, appropriate metrics of performance that can stand up to rigorous evaluation and professional scrutiny.

The authors mention the limitations of current haptic devices and illustrate with the results in their work on measuring the loads encountered in pedicle screw placement. Current, commercially available haptic devices typically provide about 1 lb of force, whereas approximately 15 lb of force are experienced during screw placement in the authors' work. Our research in drilling fresh frozen cadaver skulls showed that forces as high as 30 lb can be experienced. To approach the forces and torques we measured, however, we needed to develop a custom haptic device using augmented off-the-shelf haptic devices. We expect that the availability of haptic devices having sufficient force/torque capacity and adequate range of movement and orientation will remain a major challenge for simulators that focus on high-load situations such as bone drilling.

A final consideration is the mixture of soft-tissue-centric lower-force actions with bone-centric high-load actions in the same simulation. Typically, soft-tissue simulations are modeled with finite-element methods centered on deformation and transection, whereas bone-centric simulations are done with voxel-based techniques in which the goal is often to remove bone through an energy-based methodology that represents the action of drill or saw blades. These techniques are quite different from one another, as are the haptic interface requirements. To our knowledge, no simulator has been produced to date that supports interaction with both soft tissue and bone in the same user experience. This limitation calls for attention to how procedural subtasks are deconstructed if combined soft-tissue–bone actions are encountered, which is not uncommon in spinal procedures.

Malone and colleagues are to be congratulated for taking on an important and largely unaddressed area. Much work lies ahead in the years to come, however, before the potential of such simulators is realized.

**Dwight Meglan**
**Howard R. Champion**
*Silver Spring, Maryland*

1. Malone HR, Syed ON, Downes MS, D'Ambrosio AL, Quest DO, Kaiser MG. Simulation in neurosurgery: a review of computer-based simulation environments and their surgical applications. *Neurosurgery*. 2010;67(4):1105-1116.

10.1227/NEU.0b013e318210f038

## In Reply:

We appreciate the remarks of Drs Meglan and Champion of SimQuest, LLC. They are right to emphasize the limitations of many available haptic interfaces in reproducing the torques and loads encountered in the operative theater. The difficulty of simultaneously modeling finite-element–based soft-tissue deformation and voxel-based bone (hard-tissue) drilling, a challenge inherent to spine surgery simulation, is also addressed. Collaboration with simulation firms like SimQuest that possess the technical expertise to customize standard haptic interfaces and merge tissue deformation modalities is

essential to the continued evolution of computer-based neurosurgery simulation.

Hani Malone
Omar Syed
Michael Kaiser
*New York, New York*

10.1227/NEU.0b013e3182127c00

## Relationship Between Decompressive Craniectomy and Hydrocephalus

To the Editor:

We read with great interest the article by Rahme et al[1] in which the authors reviewed the records of 17 patients with stroke-related increased intracranial pressure who underwent decompressive craniectomy (DC). The authors described a 0% rate of shunting after DC and concluded that hydrocephalus does not frequently occur after DC. On the other hand, in the series of Waziri et al,[2] hydrocephalus developed in 15 of 17 patients after DC, and 5 required shunting after cranioplasty. Rahme et al[1] speculated that the explanation for this discrepancy might lie in the definition of hydrocephalus and the indications for shunting.

We completely agree with the viewpoint of Rahme et al[1]; however, we wish to provide further comment on this issue. Bogousslavsky and Regli[3] reported that, in 60 cases of internal carotid artery occlusion, the occurrence of ventricular dilation was related to the volume of infarction. Additionally, Barber et al[4] reported that hydrocephalus was present in 22% of patients who had a large middle cerebral artery infarction, and they received conventional medical therapy (without surgery).

Therefore, we believe that the possibility of hydrocephalus developing in the course of a large infarction should be considered. From this viewpoint, we consider that an additional explanation for the discrepancy between the results of Rahme et al[1] and Waziri et al[2] might be differences in the area and volume of the infarction. Indeed, in the Waziri et al series, all 4 patients with internal carotid artery infarction developed hydrocephalus after DC (half required shunting), and none of the 7 patients with middle cerebral artery infarction received shunting, whereas the Rahme et al series included no patients with internal carotid artery infarction.[1]

Satoru Takeuchi
Naoki Otani
Hiroshi Nawashiro
*Tokorozawa, Saitama, Japan*

1. Rahme R, Weil AG, Sabbagh M, Moumdjian R, Bouthillier A, Bojanowski MW. Decompressive craniectomy is not an independent risk factor for communicating hydrocephalus in patients with increased intracranial pressure. *Neurosurgery.* 2010;67(3):675-678.
2. Waziri A, Fusco D, Mayer SA, McKhann GM II, Connolly ES Jr. Postoperative hydrocephalus in patients undergoing decompressive hemicraniectomy for ischemic or hemorrhagic stroke. *Neurosurgery.* 2007;61(3):489-493.
3. Bogousslavsky J, Regli F. Obstruction of the internal carotid artery and cerebral malacias: tomodensitometric factors of the prognosis in 150 cases [in French]. *Schweiz Arch Neurol Neurochir Psychiatr.* 1984;134(1):13-28.
4. Barber PA, Demchuk AM, Zhang J, et al. Computed tomographic parameters predicting fatal outcome in large middle cerebral artery infarction. *Cerebrovasc Dis.* 2003;16(3):230-235.

10.1227/NEU.0b013e3182124403

## In Reply:

We would like to thank Drs Takeuchi, Otani, and Nawashiro for their interest in our article.[1] However, we find that the 2 studies they are referring to do not really lend support to their hypothesis that the divergence between our results and those of Waziri et al[2] lies in the difference in patient characteristics, specifically the extent of infarction.

In the article of Bogousslavsky and Regli,[3] the authors analyzed the development of unilateral ipsilateral ventricular dilation and cortical atrophy in patients with large strokes secondary to internal carotid artery occlusion or stenosis. There was no mention of hydrocephalus in their report. It is important to distinguish between true hydrocephalus, that is, mismatch between CSF production and resorption, and ventricular dilation or hydrocephalus ex vacuo, which is merely a radiological finding caused by large areas of neuronal loss and encephalomalacia after a massive infarction.

In their publication, Barber et al[4] sought to determine early CT signs predictive of death after large middle cerebral artery (MCA) infarction in a large cohort of conservatively managed patients, none of which had undergone decompressive craniectomy. The authors found that moderate or severe hydrocephalus was predictive of death on univariate, but not multivariate analysis. It must be noted, however, that these authors were referring to acute obstructive hydrocephalus, a complication of cerebral edema-related mass effect in large ischemic strokes. Conversely, in our study[1] and that of Waziri et al,[2] patients were typically protected against obstructive hydrocephalus by the wide surgical decompression. Rather, the incidence of chronic communicating hydrocephalus in survivors of malignant MCA territory infarction and other types of stroke was assessed.

To the best of our knowledge, there is no direct relationship between communicating hydrocephalus and ischemic stroke. Additionally, in our experience, hydrocephalus is not a frequent complication of decompressive craniectomy.[1] Therefore, unless new scientific evidence comes to disprove these findings, we have no reason to believe that hydrocephalus should be a major concern in the management of patients with large MCA or internal carotid artery infarctions.

Ralph Rahme
Alexander G. Weil
Michel W. Bojanowski
*Montreal, Quebec, Canada*

1. Rahme R, Weil AG, Sabbagh M, Moumdjian R, Bouthillier A, Bojanowski MW. Decompressive craniectomy is not an independent risk factor for communicating hydrocephalus in patients with increased intracranial pressure. *Neurosurgery*. 2010;67(3):675-678.
2. Waziri A, Fusco D, Mayer SA, McKhann GM II, Connolly ES Jr. Postoperative hydrocephalus in patients undergoing decompressive hemicraniectomy for ischemic or hemorrhagic stroke. *Neurosurgery*. 2007;61(3):489-494.
3. Bogousslavsky J, Regli F. Obstruction of the internal carotid artery and cerebral malacias. Tomodensitometric factors of the prognosis in 150 cases [French]. *Schweiz Arch Neurol Neurochir Psychiatr*. 1984;134(1):13-28.
4. Barber PA, Demchuk AM, Zhang J, et al. Computed tomographic parameters predicting fatal outcome in large middle cerebral artery infarction. *Cerebrovasc Dis*. 2003;16(3):230-235.

10.1227/NEU.0b013e3182127bdc

J Neurosurg 114:1715–1722, 2011

# Real-time control of a prosthetic hand using human electrocorticography signals

## Technical note

Takufumi Yanagisawa, M.D., Ph.D.,[1,2] Masayuki Hirata, M.D., Ph.D.,[1] Youichi Saitoh, M.D., Ph.D.,[1] Tetsu Goto, M.D., Ph.D.,[1] Haruhiko Kishima, M.D., Ph.D.,[1] Ryohei Fukuma, M.S.,[2,3] Hiroshi Yokoi, Ph.D.,[4] Yukiyasu Kamitani, Ph.D.,[2,3] and Toshiki Yoshimine, M.D., Ph.D.[1]

[1]*Department of Neurosurgery, Osaka University Medical School, Osaka;* [2]*ATR Computational Neuroscience Laboratories, Kyoto;* [3]*Nara Institute of Science and Technology; and* [4]*Department of Precision Engineering, University of Tokyo, Japan*

*Object.* A brain-machine interface (BMI) offers patients with severe motor disabilities greater independence by controlling external devices such as prosthetic arms. Among the available signal sources for the BMI, electrocorticography (ECoG) provides a clinically feasible signal with long-term stability and low clinical risk. Although ECoG signals have been used to infer arm movements, no study has examined its use to control a prosthetic arm in real time. The authors present an integrated BMI system for the control of a prosthetic hand using ECoG signals in a patient who had suffered a stroke. This system used the power modulations of the ECoG signal that are characteristic during movements of the patient's hand and enabled control of the prosthetic hand with movements that mimicked the patient's hand movements.

*Methods.* A poststroke patient with subdural electrodes placed over his sensorimotor cortex performed 3 types of simple hand movements following a sound cue (calibration period). Time-frequency analysis was performed with the ECoG signals to select 3 frequency bands (1–8, 25–40, and 80–150 Hz) that revealed characteristic power modulation during the movements. Using these selected features, 2 classifiers (decoders) were trained to predict the movement state—that is, whether the patient was moving his hand or not—and the movement type based on a linear support vector machine. The decoding accuracy was compared among the 3 frequency bands to identify the most informative features. With the trained decoders, novel ECoG signals were decoded online while the patient performed the same task without cues (free-run period). According to the results of the real-time decoding, the prosthetic hand mimicked the patient's hand movements.

*Results.* Offline cross-validation analysis of the ECoG data measured during the calibration period revealed that the state and movement type of the patient's hand were predicted with an accuracy of 79.6% (chance 50%) and 68.3% (chance 33.3%), respectively. Using the trained decoders, the onset of the hand movement was detected within 0.37 ± 0.29 seconds of the actual movement. At the detected onset timing, the type of movement was inferred with an accuracy of 69.2%. In the free-run period, the patient's hand movements were faithfully mimicked by the prosthetic hand in real time.

*Conclusions.* The present integrated BMI system successfully decoded the hand movements of a poststroke patient and controlled a prosthetic hand in real time. This success paves the way for the restoration of the patient's motor function using a prosthetic arm controlled by a BMI using ECoG signals. *(DOI: 10.3171/2011.1.JNS101421)*

**Key Words** • **brain-machine interface** • **prosthetic hand** • **electrocorticography signal** • **real time** • **support vector machine**

There are several diseases and conditions that lead to a loss of muscle control without disruption of the patients' cognitive abilities. These include amyotrophic lateral sclerosis, brainstem stroke, spinal cord injury, muscular dystrophy, and cerebral palsy. Brain-machine interface technology can offer these patients greater independence and a higher quality of life, providing the individual with control of external devices with which to communicate with others and manipulate their environment according to their will.[29]

Several signal platforms could be used as input signals for BMIs in a clinical setting: EEG,[30] MEG,[27] neuronal ensemble activity recorded intracortically (single units)[8,9,28] and/or local field potentials,[1,15] and ECoG.[14,18,21] Each type of signal has proven to be useful for BMIs, although each has advantages and disadvantages regarding utility in an applied setting. Although EEG and MEG

*Abbreviations used in this paper:* BMI = brain-machine interface; ECoG = electrocorticography; EEG = electroencephalography; EMG = electromyography; FFT = fast Fourier transform; MEG = magnetoencephalography; SVM = support vector machine.

signals can be measured noninvasively,[30] they have low spatial resolution compared with the other signals and are susceptible to artifacts from other sources.[7] Single-unit recordings have been shown to convey large amounts of information for the successful control of a prosthetic arm in a self-feeding task of monkeys.[26] This type of BMI system has already been applied to paralyzed patients,[9] but the clinical implementation of intracortical BMIs is currently impeded by difficulty in maintaining stable long-term recordings and the substantial technical requirements of the recordings.[6,22] Electrocorticography has a higher spatial resolution and better signal-to-noise ratio than EEG or MEG. Its signals have been used to control the movement of a cursor on a computer screen,[21] to reconstruct the trajectory of a 2D arm movement,[18] and to decode a single finger movement.[16] Moreover, ECoG recordings have superior long-term stability than intracortical single-unit recordings, as well as lower technical difficulty and clinical risk.[4] Even though ECoG signals have been shown to be useful for BMI systems, they have not been used to control the movement of a prosthetic hand. Here, we propose an integrated BMI system to control the movement of a prosthetic hand using ECoG signals generated while the patient moved his hand.

Previously, we developed a system in which a patient's EMG signals were used to control the movement of a prosthetic hand.[12,17] This system records the EMG signals and converts them into a power spectrum to classify some simple movements. The user can control the prosthetic hand by performing or attempting to perform simple hand movements, such as hand grasping, hand opening, and making a scissor shape. By combining such simple movements, an amputee was able to use the prosthetic hand for writing by holding a pen, cooking by grasping a kitchen knife, and other activities of daily living.[32] In the present study, we removed the EMG sensors and control unit from this system and attached a new unit that records and classifies ECoG signals to control the prosthetic hand. The new integrated system was designed to classify some simple movements using only 3 frequency power bands of the ECoG signals.

With the new integrated system, the ECoG signals of a stroke patient were recorded when he performed 3 types of hand movements. Time-frequency analysis of the signals demonstrated that 3 frequency power bands contained the characteristic features relating to the movements. With these features, the state and the type of movement were inferred by 2 decoders. The decoding accuracy was compared among the 3 frequency bands to identify the most informative band. With the 2 decoders, the freely performed movements were inferred so that the prosthetic hand faithfully mimicked the individual's hand in real time.

## Methods

### *Patient*

This 64-year-old man with thalamic pain on the left side of his body participated in this study. He had incomplete left hemiparesis due to a right thalamic hemorrhage 7 years earlier. He was barely able to perform simple hand movements (grasping, opening, and making a scissor shape). Subdural electrodes had been implanted on the right sensorimotor cortex to reduce intractable pain by delivering electrical stimulation.[10] First, 2 sheets of a 30-electrode array were temporarily implanted on a broad cortical area around his hand motor strip to determine an optimal stimulation site where the maximum reduction of his pain was achieved. The number and location of the electrodes were chosen to stimulate the cortical area corresponding to the body parts with pain. These electrodes were implanted for 2 weeks. Then, after the optimal site was determined, an array of 4 electrodes was implanted at the optimal site for chronic stimulation to reduce the pain. The patient participated in our study during the 2 weeks of temporary electrode placement. He was informed of the purpose and possible consequences of this study, and written informed consent was obtained. The ethics committee of Osaka University Hospital approved the present study.

### *Prosthetic Hand*

The prosthetic hand was an experimental anthropomorphic hand developed by Dr. Yokoi.[12] The general movement mechanisms and degrees of freedom of the hand mimicked those of a human hand. The hand was equipped with 8 DC motors to independently actuate 8 individual tendons of the hand. The 8 tendons work in a coordinated manner to accomplish flexion or extension of each individual finger. The commands to the hand were updated by the host computer system every 200 msec.

### *Recording Methods*

Sixty planar-surface platinum grid electrodes (2 sheets of a 5 × 6 array, Unique Medical Co.) were placed over the patient's right sensorimotor cortex (see Fig. 2A). The electrodes had a diameter of 3 mm and a center-to-center interelectrode distance of 7 mm. Video recording was performed during experiments. Electromyography recordings of the contralateral flexor digitorum superficialis muscle were collected at the same time. The video and EMG recordings were not used for the decoding but were used to identify the onset of the actual movement during offline analysis.

The location of the implanted electrodes was identified by standard neurosurgical techniques, both anatomically and electrophysiologically. After induction of general anesthesia, we performed a frontoparietal craniotomy over the sensorimotor cortex. The location of the central sulcus was estimated using preoperative MR imaging and confirmed by the phase reversal of the N20 component of the intraoperative somatosensory evoked potentials.

### *Movement Tasks*

Experiments were performed in an electromagnetically shielded room approximately 1 week after electrode placement. The patient was instructed to perform 3 types of movements with his left hand: a grasping motion, a hand-opening motion, and a scissor-shape motion (extension of the second and third fingers). He selected and

performed 1 of the 3 hand movements immediately after the presentation of a sound cue that recurred every 5.5 seconds (calibration period [Fig. 1A]). The sound cue was delivered from a loudspeaker controlled by Matlab 2007b (Mathworks), consisting of 3 beeps presented every 1 second. The patient was instructed to move his hand just after the third sound and to return his hand to a resting position immediately after the movement. For the resting position, the patient was instructed to relax his hand while slightly flexing his fingers. The 3 types of movement were performed approximately 40 times each. This calibration period took approximately 20 minutes with some breaks in between. During this period, there was no training of the patient.

After the calibration period with the external cues, the patient performed the same task at self-paced intervals without any external cues (free-run session [Fig. 1B]). The free-run session lasted for approximately 20 minutes with some breaks. Therefore, all of the experiments in this study took only approximately 1 hour. Notably, the patient performed the free-run task without training to control the prosthetic hand; indeed, it was only necessary to train the decoder to the ECoG signals obtained in the calibration period (see the *Decoding Algorithms* section for details).

*Data Collection and Preprocessing*

Electrocorticography signals were measured using a 128-channel digital EEG system (EEG 2000, Nihon Koden Corp.) and digitized at a sampling rate of 1000 Hz. All subdural electrodes were referenced to a scalp electrode placed on the nasion. The bandpass filter for the data analysis was set to 0.16–300 Hz.

At first, during the calibration period, the ECoG signals of all implanted electrodes were examined for 4000 msec in each session (–2000 to 2000 msec from the cue onset of each movement). A time-frequency analysis of the ECoG signals was performed using EEGLAB v5.03.[5] The power spectrum of the ECoG signals was analyzed for each electrode and each type of movement. From the results of the power spectrum, we identified 3 frequency power bands with characteristic modulation during the movement tasks: 1–8, 25–40, and 80–150 Hz

For the decoding analysis, the ECoG signals of all implanted electrodes were obtained by reference to the 3 beeps. Figure 1A shows the duration of the ECoG signals used for the decoding analysis: "N," ECoG signals of 1 second after the first sound; "R," ECoG signals of 1 second after the second sound; and "M," ECoG signals of 1 second after the third sound. An FFT algorithm was performed for each 1-second signal to obtain the 3 frequency power bands (1–8, 25–40, and 80–150 Hz). The FFT was performed using EEGLAB v5.03. For each trial and electrode, the R and M frequency power bands were normalized by dividing them with the corresponding power of N. The normalized M and R power bands were used as the input features for the following decoding analysis (Fig. 1A).

In the free-run session, the 1-second ECoG signals were recorded online every 200 msec. The FFT algorithm was performed for each 1-second signal to obtain the 3 frequency power bands for each electrode. The frequency power bands of each electrode were divided by the corresponding power bands of the baseline features (baseline features were defined as the mean frequency power bands of N that were obtained by averaging the features of N for all trials in the calibration period).

*Decoding Algorithms*

With the features obtained in the calibration period, we constructed 2 decoders, or linear classifiers, to infer the patient's movements on a trial-by-trial basis. The decoders were trained or calculated using mathematical algorithms to infer the patient's movements using only a novel ECoG signal. The normalized powers of the 3 frequency bands (features) were used to train the 2 decoders based on the linear SVM.[31] Decoder 1 was trained to classify the movement state R or M, with the features of R and M (Fig. 1A). Decoder 2 was trained to predict the types of performed movement with the features of M (Fig. 1A). The mathematical details of these decoders are described in the supplementary section and the following references (http://www.cns.atr.jp/dni/en/downloads/brain-decoder-toolbox).[11,31]

The decoding accuracy was compared among the decoding of each of the 3 frequency bands to identify the most informative frequency band. The decoding accuracy was estimated by using a 5-fold cross-validation method *(Appendix)*.

*Real-Time Decoding and Prosthetic Hand Control*

The 2 decoders trained by the ECoG signals with the external cues were applied to the novel ECoG signals in real time. Decoder 1 classified the ECoG signals as either R or M to infer the onset of movement. When the inferred state changed from R to the two successive M decoder results, movement onset was inferred (or defined) as the time between R and M. Then, Decoder 2 classified the type of movement using the feature of the second M (Fig. 1B).

According to the decoding results, the prosthetic hand was controlled to mimic the patient's movements. When the decoding result from Decoder 1 was R, the prosthetic hand was moved to the predefined resting position. When movement onset was inferred by Decoder 1, then Decoder 2 inferred the type of movement using the current ECoG signals. Then, the prosthetic hand was moved to the predefined posture of the inferred movement. The posture was maintained for 1 second, regardless of the decoding results from Decoder 1. After 1 second, the prosthetic hand was moved back to the resting position.

## Results

*Offline Time-Frequency Analysis*

During the movements in the calibration period, the power spectrum of the ECoG signals on the sensorimotor cortex varied consistently. Figure 2B illustrates an example of the power spectrum time locked to the external sound cue during the grasping movement. The signal was recorded from an electrode on the primary motor cortex

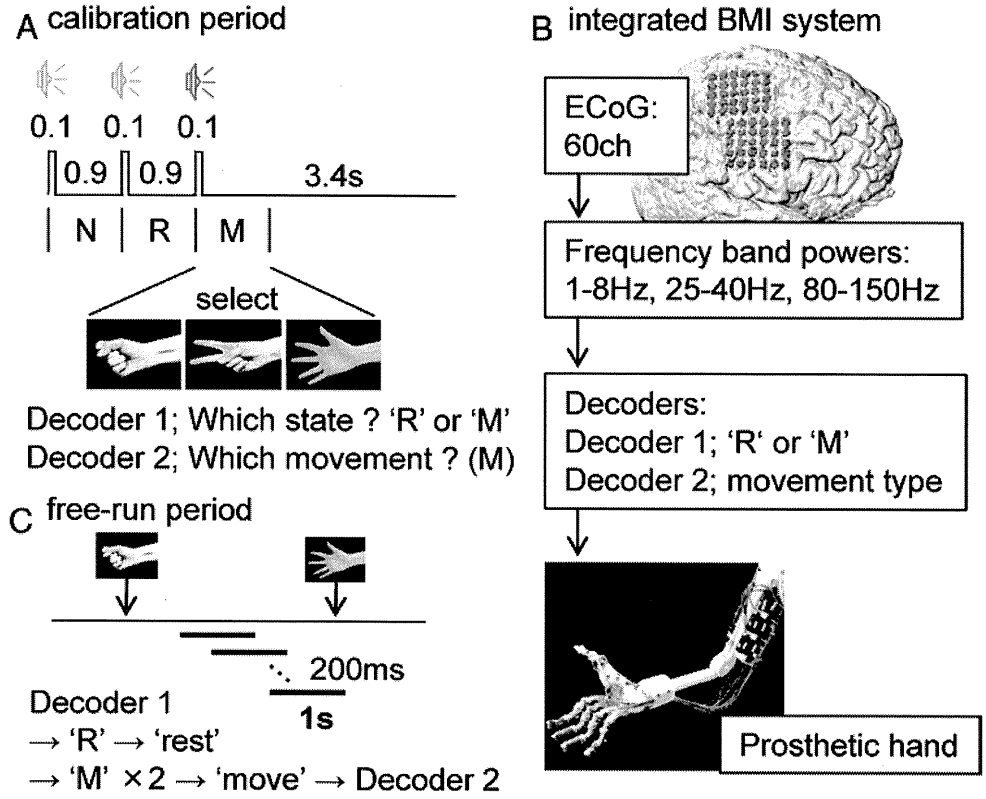


FIG. 1. Illustrations of the task and the integrated real-time decoding system. **A:** The task in the calibration period. The 1-second ECoG signals after each sound were defined as: 1st, "N" for normalization; 2nd, "R" for resting state; and 3rd, "M" for moving state. Decoders 1 and 2 were trained with the R + M and M ECoG signals, respectively. The representative photographs of hands show the task movements performed by a healthy individual. **B:** The task in the free-run period. The 1-second ECoG signals obtained every 200 msec were classified by Decoders 1 and 2 when the patient performed 1 of the 3 hand movements with arbitrary timing. **C:** Illustration of the integrated BMI system.

indicated by a blue arrow in Fig. 2A. As shown in Fig. 2B, the power reduction of the beta band (25–40 Hz) (event-related desynchronization) and the power increase of the theta (1–8 Hz) and gamma (80–150 Hz) bands (event-related synchronization) were observed around the movement onset. These frequency features, event-related desynchronization and event-related synchronization, were observed consistently on the sensorimotor cortex during the movement task.

The spatial distribution of these features on the electrodes differed depending on the movement (Fig. 2C). The increase in the power of the gamma and theta bands was observed at the localized area of the primary motor cortex. However, the decrease in the power of the beta band was observed diffusely around the primary motor cortex (Fig. 2C). The spatial distribution of each frequency power band differed among the 3 types of movement, especially for the gamma and theta bands. We selected these 3 frequency power bands as the input features for decoding.

*Offline Analysis of Decoding*

The patient's hand movement was inferred by the decoders using the frequency features of the ECoG signals on a trial-by-trial basis. Offline cross-validation analysis of the ECoG data measured during the calibration period revealed that the patient's state and the movement type were predicted with an accuracy of 79.6% (chance 50%) and 68.3% (chance 33.3%), respectively (Fig. 3). Among the 3 frequency bands, the gamma band power exhibited the best performance for the decoding of both the states and types of movement (Fig. 3).

Next, the trained Decoder 1 was tested to determine whether it could detect the onset of movement on a trial-by-trial basis. For the calibration period, the 1-second ECoG signals were classified using Decoder 1 for every 200 msec from −2 to 2 seconds relative to the onset cue. As shown in Fig. 4 left, the inferred rate of M was low before the onset cue and high after the cue. When we defined the onset as the time Decoder 1 inferred 2 successive M results after R, the movement onset was frequently inferred just after the actual onset cue (Fig. 4 right). Notably, 88% of the inferred onsets of movement were distributed between −0.5 to 0.5 seconds from the actual onset of the cue. For the calibration period, the movement onset was accurately inferred by the trained Decoder 1.

*Real-Time Prosthetic Hand Control*

Using the trained decoders, the ECoG signals were decoded in real time when the patient performed the 3 types of hand movement at an arbitrary timing (free-run period). Decoder 1 detected 61.0% of the movement onsets within 1 second from the actual onset of movement detected by the EMG signals. The mean difference be-

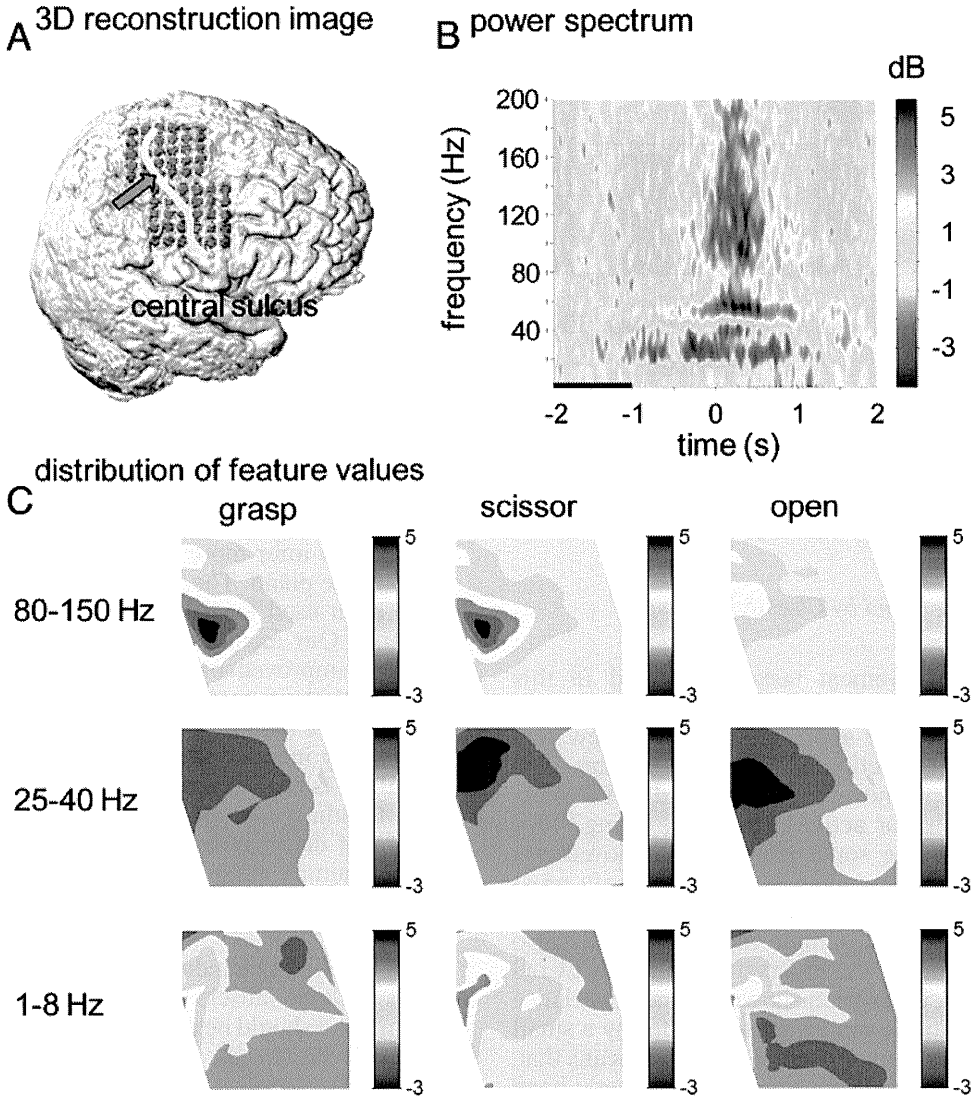


**Fig. 2.** Power spectrum of the ECoG signals during movement. **A:** Reconstructed MR image of the patient's brain with superimposed *red circles* indicating the position of the 60-channel grid electrodes. The *yellow line* indicates the location of the central sulcus. **B:** A power spectrum time locked to the external cues (Time 0 corresponds to the onset cue). The signals of the primary motor cortex (indicated by the *blue arrow* in **A**) were obtained during the grasping task. The *horizontal black line* shows the normalization period. **C:** Contour map of the mean frequency power bands. For each frequency band and each type of movement, the normalized power at 1 second after the onset of movement was averaged and shown on the location of the electrodes. The alignment of the electrode is the same as in panel **A**.

tween the inferred onset and the actual onset of movement was 0.37 ± 0.29 msec (± SD). The majority of the patient's hand movements were detected before the actual onset of movement (Fig. 5 left). However, the actual onset of movement of the prosthetic hand was delayed from the inferred onset timing due to the processing time (Video 1).

**Video 1.** A prosthetic hand (with a white glove) mimicking the patient's hand movements. The *markers* on the patient's arm were not used in the present study. Click here to view with Windows Media Player. Click here to view with Quicktime.

At the detected time, the type of movement was correctly decoded with an accuracy of 69.2%. The patient's hand movements inferred by the 2 decoders were performed by a prosthetic hand in real time (Fig. 5 right). Notably, the patient was not trained to control the prosthetic hand. The prosthetic hand was successfully controlled to faithfully mimic the patient's hand movements using only the ECoG signals without any external cues.

## Discussion

We have demonstrated that a BMI system using ECoG signals can accurately reproduce a patient's hand movements without training the patient. The system learned the features of the ECoG signals, while the post-stroke patient moved his hand naturally following sound cues. The real-time decoding of ECoG signals was then successfully performed for movements without any external cues. This is the first report describing the control of a prosthetic hand in real-time using a BMI system with ECoG signals. These successful results with a post-

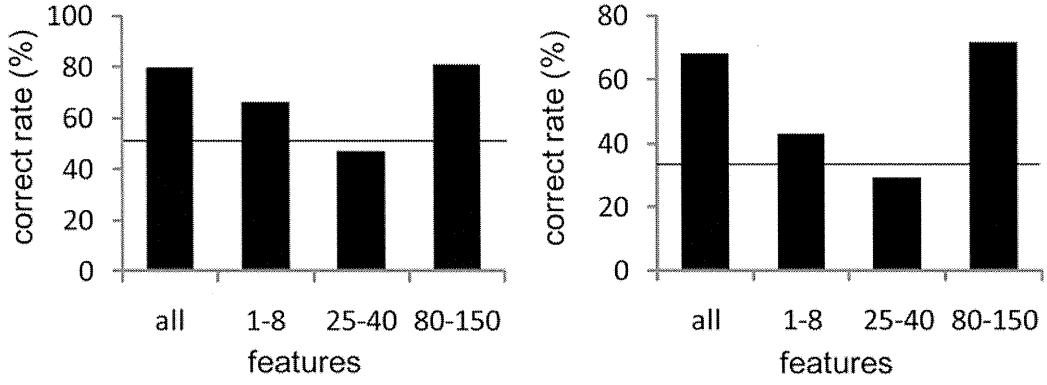


**Fig. 3.** Classification accuracy of the calibration period. The classification accuracy of the movement state **(left)** and the movement type **(right)** in the calibration period. The accuracy of the 3 frequency bands *(all)* and each single frequency band (1–8, 25–40, and 80–150 Hz) were compared. The *horizontal lines* show the chance level for each classification.

stroke patient indicate the feasibility of the clinical use of ECoG-based BMI.

*Control of Prosthetic Hand by Classifying Simple Movements*

Although the movement tasks performed in this study were simple compared with those in previous studies,[16,26] the success of our approach suggests a new way to restore the motor function of paralyzed patients. The combination of simple movements generated by the prosthetic hand is useful for activities of daily living.[32] For example, by classifying some simple hand movements with EMG signals, an amputee was able to use a prosthetic hand to improve her quality of life. This method of prosthetic control with simple movements may also be useful for controlling the prosthetic hand with ECoG signals. In addition, it has been shown that most variance in human hand postures can be accounted for by a small number of combined joint movements.[23] This means that, by combining some basic movements, a prosthetic hand could emulate most of the natural postures of a human hand. The control of a prosthetic device, by classifying some simple movements, with ECoG signals will enable a prosthetic hand to be a practical and useful device in a patient's day-to-day life.

Furthermore, ECoG signals have the potential to be decoded to infer more sophisticated movements such as playing the piano. The ECoG signals of epilepsy patients have been used to decode the movements of individual fingers.[16] Our method of controlling the prosthetic hand may be improved by using ECoG signals obtained in patients without motor dysfunction. In addition, the implantation of a high-density electrode array in the central sulcus may increase the information derived from ECoG signals. It is necessary to improve ECoG-based BMIs not only to adjust the control of a prosthetic device for activities of daily living but also to improve the ability to decode human motor representations.

*Prosthetic Control by Paralyzed Patients*

The clinical candidates for the BMI system are patients without muscle control of their limbs. Therefore, our method should be applicable in patients with complete paralysis. Previously, we showed that ECoG signals could be neurally decoded in patients with monoplegia.[31] Electrocorticography signals from the sensorimotor cortex in patients with brachial plexus avulsion were successfully decoded when the patients only intended or attempted to move their completely paralyzed upper limbs. The intention of movement was inferred accurately by a decoder

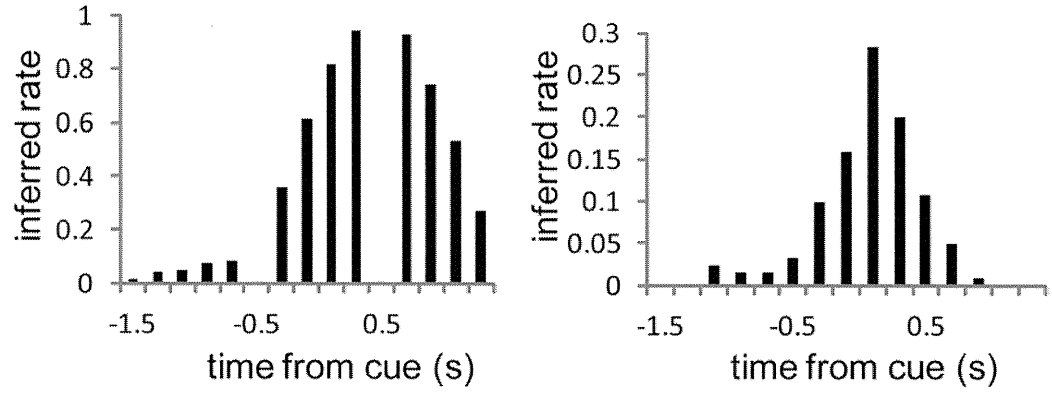


**Fig. 4. Left:** Onset timing inferred by Decoder 1 for the calibration period. The rate of M inferred by Decoder 1 using the 1-second ECoG signals sliding by 200 msec from –2 to 2 seconds. The horizontal axis shows the middle time of the 1-s ECoG signal (Time 0 corresponds to the onset cue). The *gray bars* correspond to the training data sets of Decoder 1. **Right:** The rate of onset inferred by Decoder 1.

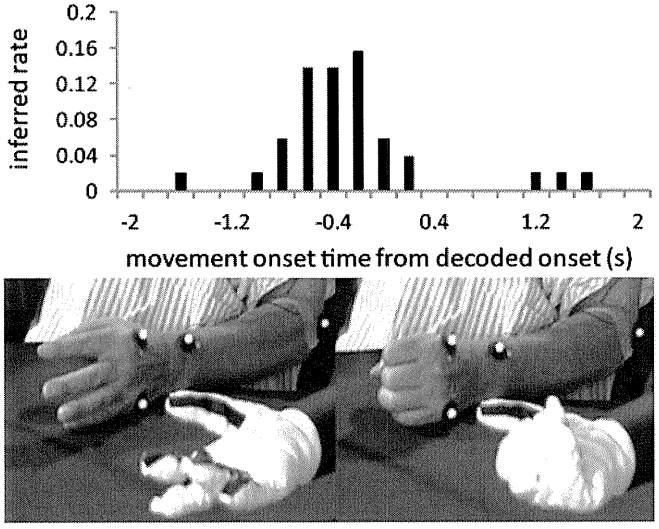


FIG. 5. Real-time decoding and prosthetic hand control with ECoG. **A:** The distribution of the actual movement onset timing from the nearest inferred onset timing by Decoder 1 (free-run period). **B:** Representative photographs of the prosthetic hand (with a white glove) controlled by the poststroke patient's ECoG signals in real time. A prosthetic hand (with a white glove) mimicked the patient's hand movements. The *markers* on the patient's arm were not used in the present study.

trained by the same method used in the present study. By using simple and common movements that can be easily planned by patients, our method may be applicable to a large number of paralyzed patients as a clinically beneficial device to restore their motor functions.

*Usefulness of ECoG Signals From the Gamma Band Power*

Decoding analysis of the ECoG signals revealed that the gamma band power was the most informative in inferring the state and type of hand movement among the 3 frequency bands. This result was consistent with previous studies in which human movements were inferred using ECoGs.[18,21] Moreover, the power increase of the gamma band correlates with the firing activities of neurons representing neural information.[19,20] Thus, the information contained within the gamma band facilitates the use of ECoG signals in a clinically applicable BMI system.

Among the currently available signal platforms for BMI, intracortical recordings have been shown to provide the largest amount of information to decode movements by using the firing activities of neurons.[24,26] However, this method is associated with difficulties in maintaining stable long-term signals and substantial technical difficulties in recording the signals. Therefore, clinical application of these signals is impeded.[13] Electrocorticography signals are superior to intracortical signals with respect to stability and durability, as demonstrated in monkeys over a 1-year period.[4] On the other hand, with noninvasive signal platforms, such as EEG and MEG, it is difficult to record the gamma band power on a trial-by-trial basis.[27] With ECoG, the gamma band power is consistently available to infer movements on a trial-by-trial basis and may be recorded for a much longer time than intracortical recordings. Therefore, although ECoG is an invasive recording technique, it provides a promising signal that could be used for a BMI in the clinical setting.

## Conclusions

The real-time decoding of the ECoG signal using the gamma band power was applied successfully to allow a paralyzed patient to control a prosthetic hand. This success may lead to the development of a clinically feasible BMI system that uses the safe and stable ECoG signals. Our method of using the combination of simple movements paves the way for the restoration of motor function in paralyzed patients using a prosthetic arm controlled by a BMI through ECoG signals.

### Disclosure

This work was supported in part by the Strategic Research Program for Brain Sciences of MEXT, Grants-in-Aid for Scientific Research (no. 22700435) from JSPS, Nissan Science Foundation, the Ministry of Health, Labor and Welfare (no. 18261201), and the SCOPE, SOUMU.

Author contributions to the study and manuscript preparation include the following. Conception and design: Hirata, Yanagisawa, Kamitani. Acquisition of data: Hirata, Yanagisawa, Goto, Fukuma. Analysis and interpretation of data: Hirata, Yanagisawa, Kamitani. Drafting the article: Yanagisawa. Critically revising the article: Hirata. Reviewed final version of the manuscript and approved it for submission: all authors. Statistical analysis: Yanagisawa. Administrative/technical/material support: Hirata, Saitoh, Goto, Kishima, Fukuma, Yokoi, Kamitani, Yoshimine. Study supervision: Hirata, Kamitani, Yoshimine.

### Appendix

*Construction of the Decoders*

The decoder is a mathematical algorithm used to calculate a linearly weighted sum of the features $x = (x_1, x_2, \cdots, x_N)$ plus a bias for each class of movement ("linear detector function," $g_{class}(x)$). In the equation, $x_i$ corresponds to the $i$-th feature of N features, $w_{i,class}$ is the weight of the $i$-th feature, and $w_{0,class}$ is the bias. Here, each feature corresponds to a certain frequency band power for each electrode. That is, 3 (frequency bands) × 60 (electrodes) = 180 features that were used for this calculation. The weights $w_{0,class}$ and $w_{i,class}$ were determined for each class of movement such as grasping, opening, and scissor-shape hands.

$$g_{class}(x) = w_{0,class} + \sum_{j=1}^{N} w_{i,class} \times x_i$$

The class with the maximum value of $g_{class}(x)$ was chosen as the predicted movement class.[11,31] In the case of Decoder 1, the class corresponds to 1 of 2 states: R or M. For Decoder 2, the class corresponds to 1 of 3 types of movement: grasping, opening, and scissor-shape hand movements. The selected class indicated the predicted movement state or movement type.

Individual weights and biases for each class were determined using the linear SVM applied to a training data set.[25] First, the SVM algorithm was applied to each pair of class. The discriminant function, $g_{i,j}(x)$ for the discrimination of Class i and j, is expressed by a weighted sum of the features plus the bias. Using a training data set, a linear SVM finds the optimal weight and bias for the discriminant function. The pairwise discriminant functions comparing Class i and the other classes were simply added to yield the linear detector function:

$$g_i(x) = \sum_{m \neq i} g_{i,m}(x)$$

The SVM algorithm was implemented using Matlab 2007b.

*Fivefold Cross-Validation*

To test the generalization of the decoders, we used 5-fold

cross-validation as a performance measure.[2,3] We randomly divided the trials into 5 blocks, using 4 for training and 1 for testing. We then used all of the training data to train the classifier and evaluated its performance on the test data. This routine was repeated 5 times, and the averaged correct percentage over all runs is presented as a measure of decoder performance.

## References


1. Andersen RA, Musallam S, Pesaran B: Selecting the signals for a brain-machine interface. **Curr Opin Neurobiol 14:**720–726, 2004
2. Bengio Y, Grandvalet Y: No unbiased estimator of the variance of K-fold cross-validation. **J Mach Learn Res 5:**1089–1105, 2004
3. Breiman L: Heuristics of instability and stabilization in model selection. **Ann Stat 24:**2350–2383, 1996
4. Chao ZC, Nagasaka Y, Fujii N: Long-term asynchronous decoding of arm motion using electrocorticographic signals in monkeys. **Front Neuroengineering 3:**3, 2010
5. Delorme A, Makeig S: EEGLAB: an open source toolbox for analysis of single-trial EEG dynamics including independent component analysis. **J Neurosci Methods 134:**9–21, 2004
6. Donoghue JP, Nurmikko A, Friehs G, Black M: Development of neuromotor prostheses for humans. **Suppl Clin Neurophysiol 57:**592–606, 2004
7. Fujiwara Y, Yamashita O, Kawawaki D, Doya K, Kawato M, Toyama K, et al: A hierarchical Bayesian method to resolve an inverse problem of MEG contaminated with eye movement artifacts. **Neuroimage 45:**393–409, 2009
8. Georgopoulos AP, Schwartz AB, Kettner RE: Neuronal population coding of movement direction. **Science 233:**1416–1419, 1986
9. Hochberg LR, Serruya MD, Friehs GM, Mukand JA, Saleh M, Caplan AH, et al: Neuronal ensemble control of prosthetic devices by a human with tetraplegia. **Nature 442:**164–171, 2006
10. Hosomi K, Saitoh Y, Kishima H, Oshino S, Hirata M, Tani N, et al: Electrical stimulation of primary motor cortex within the central sulcus for intractable neuropathic pain. **Clin Neurophysiol 119:**993–1001, 2008
11. Kamitani Y, Tong F: Decoding the visual and subjective contents of the human brain. **Nat Neurosci 8:**679–685, 2005
12. Kato R, Yokoi H, Arieta AH, Yu W, Arai T: Mutual adaptation among man and machine by using f-MRI analysis. **Robot Auton Syst 57:**161–166, 2009
13. Leuthardt EC, Schalk G, Moran D, Ojemann JG: The emerging world of motor neuroprosthetics: a neurosurgical perspective. **Neurosurgery 59:**1–14, 2006
14. Leuthardt EC, Schalk G, Wolpaw JR, Ojemann JG, Moran DW: A brain-computer interface using electrocorticographic signals in humans. **J Neural Eng 1:**63–71, 2004
15. Mehring C, Rickert J, Vaadia E, Cardosa de Oliveira S, Aertsen A, Rotter S: Inference of hand movements from local field potentials in monkey motor cortex. **Nat Neurosci 6:**1253–1254, 2003
16. Miller KJ, Zanos S, Fetz EE, den Nijs M, Ojemann JG: Decoupling the cortical power spectrum reveals real-time representation of individual finger movements in humans. **J Neurosci 29:**3132–3137, 2009
17. Nakamura T, Kita K, Kato R, Matsushita K, Hiroshi Y: Control strategy for a myoelectric hand: measuring acceptable time delay in human intention discrimination. **Conf Proc IEEE Eng Med Biol Soc 2009:**5044–5047, 2009
18. Pistohl T, Ball T, Schulze-Bonhage A, Aertsen A, Mehring C: Prediction of arm movement trajectories from ECoG-recordings in humans. **J Neurosci Methods 167:**105–114, 2008
19. Quian Quiroga R, Panzeri S: Extracting information from neuronal populations: information theory and decoding approaches. **Nat Rev Neurosci 10:**173–185, 2009
20. Ray S, Crone NE, Niebur E, Franaszczuk PJ, Hsiao SS: Neural correlates of high-gamma oscillations (60-200 Hz) in macaque local field potentials and their potential implications in electrocorticography. **J Neurosci 28:**11526–11536, 2008
21. Schalk G, Miller KJ, Anderson NR, Wilson JA, Smyth MD, Ojemann JG, et al: Two-dimensional movement control using electrocorticographic signals in humans. **J Neural Eng 5:**75–84, 2008
22. Shain W, Spataro L, Dilgen J, Haverstick K, Retterer S, Isaacson M, et al: Controlling cellular reactive responses around neural prosthetic devices using peripheral and local intervention strategies. **IEEE Trans Neural Syst Rehabil Eng 11:**186–188, 2003
23. Thakur PH, Bastian AJ, Hsiao SS: Multidigit movement synergies of the human hand in an unconstrained haptic exploration task. **J Neurosci 28:**1271–1281, 2008
24. Truccolo W, Friehs GM, Donoghue JP, Hochberg LR: Primary motor cortex tuning to intended movement kinematics in humans with tetraplegia. **J Neurosci 28:**1163–1178, 2008
25. Vapnik VN: **Statistical Learning Theory.** New York: Wiley, 1998
26. Velliste M, Perel S, Spalding MC, Whitford AS, Schwartz AB: Cortical control of a prosthetic arm for self-feeding. **Nature 453:**1098–1101, 2008
27. Waldert S, Preissl H, Demandt E, Braun C, Birbaumer N, Aertsen A, et al: Hand movement direction decoded from MEG and EEG. **J Neurosci 28:**1000–1008, 2008
28. Wessberg J, Stambaugh CR, Kralik JD, Beck PD, Laubach M, Chapin JK, et al: Real-time prediction of hand trajectory by ensembles of cortical neurons in primates. **Nature 408:**361–365, 2000
29. Wolpaw JR, Birbaumer N, McFarland DJ, Pfurtscheller G, Vaughan TM: Brain-computer interfaces for communication and control. **Clin Neurophysiol 113:**767–791, 2002
30. Wolpaw JR, McFarland DJ: Control of a two-dimensional movement signal by a noninvasive brain-computer interface in humans. **Proc Natl Acad Sci U S A 101:**17849–17854, 2004
31. Yanagisawa T, Hirata M, Saitoh Y, Kato A, Shibuya D, Kamitani Y, et al: Neural decoding using gyral and intrasulcal electrocorticograms. **Neuroimage 45:**1099–1106, 2009
32. Yokoi H, Kita K, Nakamura T, Kato R, Hernandez A, Arai T: Mutually adaptable EMG devices for prosthetic hand. **The International Journal of Factory Automation, Robotics and Soft Computing 1:**74–83, 2009


Manuscript submitted August 18, 2010.
Accepted January 5, 2011.
Please include this information when citing this paper: published online February 11, 2011; DOI: 10.3171/2011.1.JNS101421.

*Supplemental online information:*
Video: http://mfile.akamai.com/21490/wmv/digitalwbc.download.akamai.com/21492/wm.digitalsource-na-regional/jns10-1421.asx (Media Player)
http://mfile.akamai.com/21488/mov/digitalwbc.download.akamai.com/21492/qt.digitalsource-global/jns10-1421.mov (Quicktime)

*Address correspondence to:* Masayuki Hirata, M.D., Ph.D., Department of Neurosurgery, Osaka University Medical School, E6 2-2 Yamadaoka Suita, Osaka, Japan. email: mhirata@nsurg.med.osaka-u.ac.jp.

PAIN® 152 (2011) 860–865

PAIN®

www.elsevier.com/locate/pain

# Deep brain stimulation of the subthalamic nucleus improves temperature sensation in patients with Parkinson's disease

Tomoyuki Maruo [a], Youichi Saitoh [a,b,*], Koichi Hosomi [a,b], Haruhiko Kishima [a], Toshio Shimokawa [c], Masayuki Hirata [a], Tetsu Goto [a], Shayne Morris [a], Yu Harada [a], Takufumi Yanagisawa [a], Mohamed M. Aly [a], Toshiki Yoshimine [a]

[a] Department of Neurosurgery, Osaka University Graduate School of Medicine, Osaka, Japan
[b] Department of Neuromodulation and Neurosurgery, Center for Advanced Science and Innovation, Osaka University, Osaka, Japan
[c] Department of Ecosocial System Engineering, Graduate School of Medicine and Engineering, University of Yamanashi, Yamanashi, Japan

*Sponsorships or competing interests that may be relevant to content are disclosed at the end of this article.*

ARTICLE INFO

*Article history:*
Received 4 August 2010
Received in revised form 23 November 2010
Accepted 21 December 2010

*Keywords:*
Parkinson's disease
Deep brain stimulation
Quantitative sensory testing
Cold and warm sense threshold
Cold and heat pain threshold

ABSTRACT

Patients with Parkinson's disease (PD) reportedly show deficits in sensory processing in addition to motor symptoms. However, little is known about the effects of bilateral deep brain stimulation of the subthalamic nucleus (STN-DBS) on temperature sensation as measured by quantitative sensory testing (QST). This study was designed to quantitatively evaluate the effects of STN-DBS on temperature sensation and pain in PD patients. We conducted a QST study comparing the effects of STN-DBS on cold sense thresholds (CSTs) and warm sense thresholds (WSTs) as well as on cold-induced and heat-induced pain thresholds (CPT and HPT) in 17 PD patients and 14 healthy control subjects. The CSTs and WSTs of patients were significantly smaller during the DBS-on mode when compared with the DBS-off mode ($P < .001$), whereas the CSTs and WSTs of patients in the DBS-off mode were significantly greater than those of healthy control subjects ($P < .02$). The CPTs and HPTs in PD patients were significantly larger on the more affected side than on the less affected side ($P < .02$). Because elevations in thermal sense and pain thresholds of QST are reportedly almost compatible with decreases in sensation, our findings confirm that temperature sensations may be disturbed in PD patients when compared with healthy persons and that STN-DBS can be used to improve temperature sensation in these patients. The mechanisms underlying our findings are not well understood, but improvement in temperature sensation appears to be a sign of modulation of disease-related brain network abnormalities.



## 1. Introduction

Deep brain stimulation of the subthalamic nucleus (STN-DBS) is effective in treating patients with advanced-stage Parkinson's disease (PD) [10,11]. It is particularly effective for improving motor functional impairment, a deficit that originates from altered peripheral feedback or abnormal central processing [2,9]. In addition to motor symptoms, sensory disturbances are part of the clinical picture of PD. PD patients frequently experience pain, numbness, and decreased proprioception, all of which are thought to result from deficient gating of sensory information due to basal ganglia dysfunction [8]. These sensory disturbances could be factors contributing to motor deficits [7,16]. It is important to recognize sensory disturbances because they can lead to even more serious complications and diminish quality of life.

Little is known about the effects of STN-DBS on sensory symptoms and the mechanisms by which STN-DBS alleviates sensory symptoms in PD. The effects of treating PD patients are usually assessed using the Unified Parkinson's Disease Rating Scale (UPDRS). Although the UPDRS allows appropriate evaluation of motor symptoms and functional disability, it is not suitable for evaluating sensory symptoms. Recently, sensory dysfunction has been measured for pain symptoms in PD patients using quantitative measurements [3], by electrophysiological methods, and by recording laser-evoked potentials [20]. In particular, quantitative measurement has increasingly been used for assessment of sensory thresholds in epidemiologic, clinical, and research studies [4]. Differences in thermal quantitative sensory testing (QST) are also reportedly compatible with elevations in temperature sense thresholds and pain thresholds [6]. We were therefore interested in quantitatively evaluating temperature sensations as well as pain in PD patients with the use

* Corresponding author at: Department of Neurosurgery, Osaka University Graduate School of Medicine, 2-2 Yamadaoka, Suita, Osaka 565-0871, Japan. Tel.: +81 6 6879 3652; fax: +81 6 6879 3659.
*E-mail address:* saitoh@nsurg.med.osaka-u.ac.jp (Y. Saitoh).

0304-3959/$36.00 
doi:10.1016/j.pain.2010.12.038

of thermal QST studies. The aim of our study was to quantitatively evaluate the effects of STN-DBS on temperature sensations and pain, in hopes of improving the diagnosis and treatment of PD patients. Thus, we conducted a QST study to assess the effects of STN-DBS on both temperature sensation and pain in PD patients compared with healthy control subjects.

## 2. Methods

### 2.1. Subjects

Our study involved 2 groups of subjects: 17 patients with idiopathic PD diagnosed based on the diagnostic criteria of the UK Parkinson's Disease Society Brain Bank (6 men, 11 women; mean age: 65.7 ± 3.8 years, range: 55 to 73 years) and 14 healthy control subjects (7 men, 7 women; mean age: 54.8 ± 14.0 years, range: 28 to 74 years). The latter were selected from healthy volunteers free of central nervous system disease. All patients who underwent bilateral STN-DBS at Osaka University Hospital during the period from 2001 through 2009 were included in this study. For STN-DBS, standard surgery inclusion/exclusion criteria were applied to all cases. At the time of enrollment in the study, most patients had normal intelligence as defined by a Mini-Mental State Examination score $\geqslant 25$ and correct language comprehension. UPDRS motor scores had been obtained for all patients during DBS-on and DBS-off states. Cold sense thresholds (CSTs), warm sense thresholds (WSTs), cold pain thresholds (CPTs), and heat pain thresholds (HPTs) were determined on the palms of the subjects' hands. Both the more affected and the less affected sides were assessed in PD patients. Thus, the side more affected by the disease was the side with the higher UPDRS score in the PD patients. In addition to age and sex, the following clinical variables were assessed for each patient: disease duration, Hoehn and Yahr disease stage, UPDRS motor scores during DBS-on and DBS-off states, and the DBS amplitude at study enrollment. The Ethics Committee of Osaka University Hospital approved this study, and informed consent was obtained from all participants (approval number: 09213).

### 2.2. QST protocol

QST was performed with a thermal sensory analyzer (PATHWAY Pain and Sensory Evaluation System; Medoc Ltd, Ramat Yishai, Israel). The computer driven PATHWAY system contains a metal contact plate (30 × 30 mm) that can be cooled and heated by an external Peltier element and is used to assess sensory thresholds. Peltier devices can change temperature at a predictable rate and can be used to test CSTs, WSTs, CPTs, and HPTs.

CSTs, WSTs, CPTs, and HPTs were examined in all study subjects by 1 of 2 examiners (T.M. or K.H.) who followed a standardized procedure. The testing was performed in a quiet room kept at a constant temperature (21°C to 25°C), with each subject resting comfortably in a sitting position. The 9-$cm^2$ Peltier probe was placed on the palm of the hand on the tested side and fastened with an elastic Velcro strap. The baseline temperature of the probe was 32°C, and the temperature was set to change at a rate of 1°C/s until a minimum temperature of 0°C or a maximum temperature of 51°C was reached, or until the subject pressed a response button held in their opposite hand [14,18,24]. For safety reasons, a maximum temperature of 51°C and a minimum temperature of 0°C were chosen to prevent cutaneous burns. The method of limits was used to determine all thresholds [18]. To determine CSTs, WSTs, CPTs, and HPTs, the subjects were asked to press a response button held in the opposite hand to that being tested, when cold or warm sensations and cold or hot pain sensation were respectively first perceived, starting from a baseline temperature of 32°C [23,25]. The CST and WST thresholds were defined as the absolute value of the temperature change from the baseline of 32°C at which subjects indicated their first cold or warm sensations, respectively. The CPTs and HPTs were also defined as the absolute value of the temperature change from baseline at which subjects indicated the point where a respective cold or warm temperature became painful. For each of the 4 types of threshold, the test was repeated 4 times in a uniform manner. Threshold tests began with temperature sensory thresholds for cold then warm, followed by pain thresholds for cold then heat. QSTs were first performed on the right hand and then on the left hand. The mean value from the 4 tests was taken as the threshold value. For PD patients, each test was performed bilaterally in both the DBS-on and the DBS-off state, the latter being undertaken approximately 30 minutes after the stimulator was switched off (Fig. 1). For healthy control subjects, each test was performed twice with a 30-minute interval between tests to examine the effects of repetitive QST on normal subjects.

Threshold values are expressed in degrees Centigrade. The lower the temperature (below 32°C) to which a subject responded, the greater the CST or CPT; the higher the temperature (above 32°C) to which a subject responded, the greater the WST or HPT. After the maximum or minimum temperature was reached or the subject indicated a sensory threshold by pressing the response button, the temperature automatically returned to the baseline of 32°C. The temperature was set to return at a rate of 2°C/s for temperature sensation thresholds and 8°C/s for pain thresholds. To prevent possible modulation of thermal receptors, in the case of temperature threshold measurements, the metal contact plate remained at the baseline temperature for 5 seconds before temperatures increased or decreased. In the case of pain threshold measurements, this interval was 10 seconds [24]. Before the actual tests, all subjects participated in a short training session to make sure they understood the test procedure.

### 2.3. Statistical analysis

A descriptive statistical analysis was performed on all data. Median values were used for all variables to indicate thermal thresholds. A Dunnett multiple comparisons test was used to analyze differences in test results between the PD patients and the healthy control subjects. For the PD patient group, differences in temperature sense thresholds and pain thresholds between the DBS-off and DBS-on states and between the more affected and less affected sides were analyzed with a 2-factor repeated-measures analysis of variance (ANOVA). The 1-way repeated-measures ANOVA was used to test for correlations between clinical variables and QST scores. A value of $P < .05$ was considered statistically significant. SPSS for Windows 17.0 was used for all statistical analyses (SPSS Inc., Chicago, IL, USA)

## 3. Results

### 3.1. Clinical assessment

QST data were obtained for all 17 PD patients and all 14 control subjects. Clinical characteristics of the 17 PD patients are shown in detail in Table 1. The mean duration of PD at the time of testing was 15.5 ± 5.4 years. Hoehn and Yahr stages ranged from 2 to 3. The mean UPDRS motor score was 22.0 ± 7.8 during the DBS-on state and 36.3 ± 11.8 during the DBS-off state. All patients treated with STN-DBS, levodopa, and dopamine agonists showed marked improvement in UPDRS motor scores. There were no significant correlations between the sensory threshold values and patient characteristics (age, sex, Hoehn and Yahr stage, disease duration, UPDRS score, or DBS amplitude).

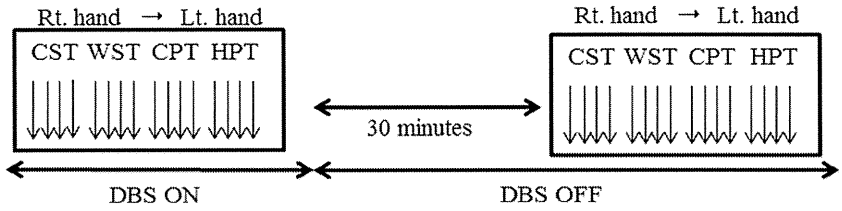


**Fig. 1.** Diagram of the QST protocol. For each type of threshold, the test was repeated 4 times, first on the right hand then on the left hand, and the mean value from the 4 tests was taken as the threshold value. For patients with PD, each test was performed both in the bilateral DBS-on state and DBS-off state (30 minutes after switching the stimulator off). CPT, cold pain threshold; CST, cold sense threshold; DBS-on, deep brain stimulation on; DBS-off, deep brain stimulation off; HPT, heat pain threshold; PD, Parkinson's disease; WST, warm sense threshold.

### *3.2. Differences in sensory thresholds between PD patients and control subjects*

CSTs and WSTs of the PD patients and control subjects are shown in Fig. 2 and Table 2. CSTs were significantly greater in PD patients in the DBS-off state than in control subjects (27.5 ± 0.8°C [less affected side] vs 30.9 ± 0.2°C [control], $P = .010$; 25.6 ± 1.0°C [more affected side] vs 30.9 ± 0.2°C [control], $P < .001$). However, CSTs did not differ significantly between PD patients in the DBS-on mode and control subjects (29.7 ± 0.3°C [less affected side] vs 30.9 ± 0.2°C [control], NS; 29.0 ± 0.6°C [more affected side] vs 30.9 ± 0.2°C [control], NS). WSTs were significantly greater in PD patients in the DBS-off state than in control subjects (36.2 ± 0.6°C [less affected side] vs 33.9 ± 0.3°C [control], $P = .013$; 36.7 ± 0.8°C [more affected side] vs 33.9 ± 0.3°C [control], $P = .002$). However, WSTs did not differ significantly between PD patients in the DBS-on state and control subjects (34.5 ± 0.3°C [less affected side] vs 33.9 ± 0.3°C [control], NS; 34.5 ± 0.3°C [more affected side] vs 33.9 ± 0.3°C [control], NS). There were no significant differences in either CPTs or HPTs between PD patients (in both DBS-on and DBS-off states) and control subjects.

### *3.3. Differences in sensory thresholds between DBS-on and DBS-off modes*

There were no significant differences in any of the thresholds of the healthy control subjects over the 2 sessions with a 30-minute interval in between (Table 3). In the patient group, there were significant differences in CSTs and WSTs between the DBS-on and DBS-off states. CSTs were significantly lower during the DBS-on state than during the DBS-off state (DBS-on 29.4°C vs DBS-off 26.6°C, $P < .001$), with a significant difference between the more affected and less affected sides (less affected side 27.3°C vs more affected side 28.6°C, $P = .020$) (Fig. 3, Table 3). WSTs were significantly lower during the DBS-on state than during the DBS-off state (DBS-on 34.5°C vs DBS-off 36.5°C, $P < .001$), with no significant difference between the more affected and less affected sides (less affected side 35.6°C vs more affected side 35.4°C). CPTs and HPTs did not differ significantly with respect to the DBS mode; however, CPTs ($P = .011$) and HPTs ($P = .016$) were significantly lower on the less affected side than on the more affected side.

## 4. Discussion

Our 2 main findings were that, firstly, significantly greater CSTs and WSTs were observed in PD patients when compared with healthy control subjects, indicating that temperature sensation is indeed impaired in PD patients. Secondly, in our patients, CSTs and WSTs were significantly reduced during the DBS-on state when compared with the DBS-off state, suggesting that STN-DBS improves temperature sensation impairments in PD patients. To our knowledge, this is the first study to quantitatively document the effects of STN-DBS on temperature sensation in PD patients.

**Table 1**
Patients with PD clinical characteristics.

| Patient no. | Age (y) | Sex | Disease duration (y) | Duration since STN DBS implant (mo) | H&Y stage | Medication (LEDD mg/d) | UPDRS motor score | | MMSE | DBS mode | DBS amplitude | |
|---|---|---|---|---|---|---|---|---|---|---|---|---|
| | | | | | | | DBS-on | DBS-off | | | Rt | Lt |
| 1 | 62 | F | 10 | 42 | 2 | 100 | 25 | 30 | 28 | Bipolar | 2.6 | 2.8 |
| 2 | 60 | F | 11 | 22 | 2 | 300 | 20 | 26 | 30 | Monopolar | 2.5 | 2.5 |
| 3 | 55 | M | 15 | 30 | 2 | 150 | 5 | 21 | 30 | Monopolar | 3.5 | 3.5 |
| 4 | 73 | F | 28 | 64 | 3 | 900 | 31 | 40 | 25 | Monopolar | 3.0 | 3.2 |
| 5 | 73 | F | 21 | 24 | 2 | 300 | 35 | 58 | 25 | Bipolar | 3.7 | 3.8 |
| 6 | 71 | M | 8 | 20 | 2 | 400 | 15 | 25 | 27 | Monopolar | 2.0 | 2.1 |
| 7 | 70 | F | 19 | 7 | 3 | 450 | 10 | 25 | 30 | Monopolar | 3.5 | 3.5 |
| 8 | 63 | F | 18 | 78 | 2 | 500 | 10 | 29 | 28 | Monopolar | 2.4 | 2.4 |
| 9 | 73 | M | 6 | 18 | 3 | 300 | 5 | 9 | 27 | Monopolar | 2.4 | 1.7 |
| 10 | 58 | M | 9 | 24 | 2 | 150 | 10 | 25 | 28 | Monopolar | 2.2 | 2.2 |
| 11 | 70 | F | 8 | 6 | 2 | 150 | 15 | 20 | 29 | Monopolar | 2.4 | 2.2 |
| 12 | 63 | F | 14 | 70 | 2 | 500 | 21 | 53 | 26 | Monopolar | 2.3 | 2.3 |
| 13 | 71 | F | 14 | 18 | 2 | 200 | 12 | 38 | 28 | Monopolar | 2.2 | 1.8 |
| 14 | 68 | M | 8 | 12 | 2 | 500 | 16 | 67 | 28 | Monopolar | 2.3 | 3.6 |
| 15 | 73 | M | 18 | 87 | 3 | 600 | 33 | 45 | 21 | Monopolar | 3.0 | 3.1 |
| 16 | 60 | F | 22 | 3 | 2 | 500 | 15 | 32 | 28 | Monopolar | 1.3 | 1.5 |
| 17 | 62 | F | 14 | 5 | 2 | 400 | 25 | 30 | 28 | Monopolar | 2.1 | 2.2 |
| Means ± SD | 65.7 ± 3.8 | | 15.5 ± 5.4 | 31.1 ± 21.8 | 2.4 ± 0.4 | 406 ± 195 | 22.0 ± 7.8 | 36.3 ± 11.8 | 27 ± 2 | | 2.5 ± 0.5 | 2.6 ± 0.6 |

LEDD, levodopa-equivalent daily dose; PD, Parkinson's disease"; H&Y, modified Hoehn and Yahr scale score"; STN, subthalamic nucleus; L-dopa, levodopa; UPDRS, unified Parkinson's disease rating scale; DBS, deep brain stimulation; MMSE, mini-mental state examination.

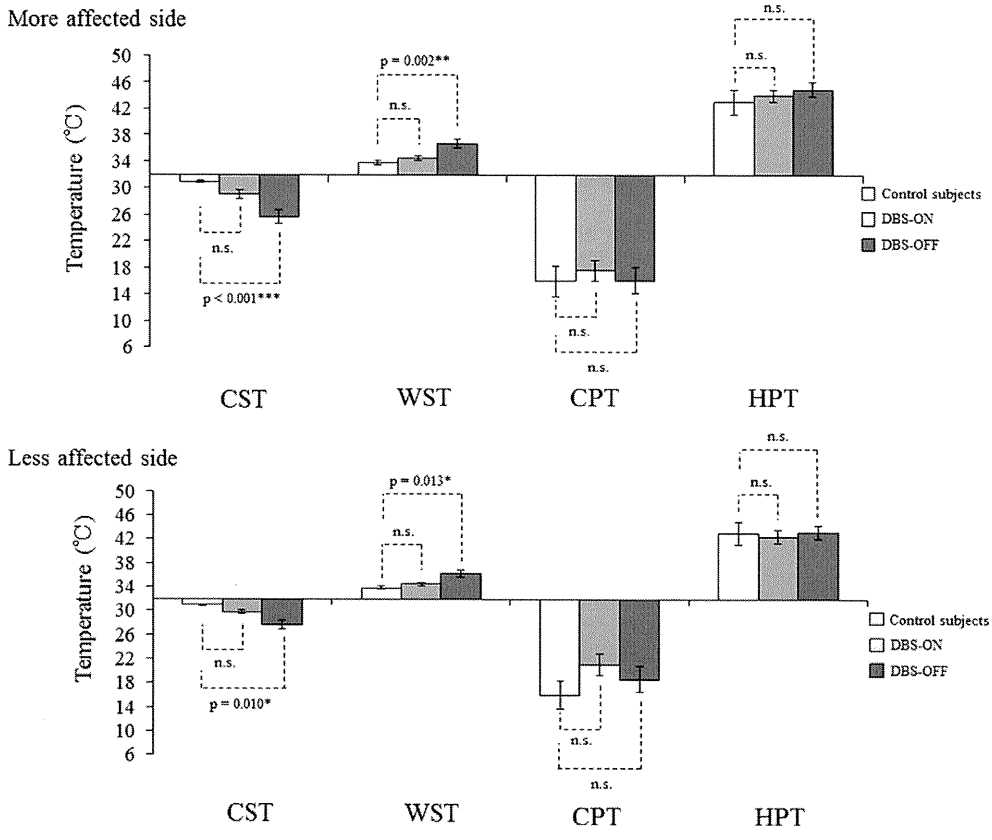


**Fig. 2.** Sensory thresholds in PD patients in the DBS-on state and DBS-off state compared with healthy control subjects. CSTs and WSTs were significantly greater in PD patients in the DBS-off state than in the healthy control subjects. Sensory threshold values are expressed in degrees Celsius. Mean values are shown (error bars represent SEM). A *P* value of <.05 was considered statistically significant (**P* < .05; ***P* < .01; ****P* < .001; NS, *P* > .05). CPT, cold pain threshold; CST, cold sense threshold; DBS-on, deep brain stimulation on; DBS-off, deep brain stimulation off; HPT, heat pain threshold; PD, Parkinson's disease; WST, warm sense threshold.

Sensory disturbances, which can either accompany or precede PD-associated motor disorders, are part of the clinical picture of PD and are most frequent in PD cases with motor complications [21]. It has been recommended that thermal QST for temperature sensation and pain are incorporated into routine neurological assessments [23]. QST of thermal modalities has been reported suitable for the screening and long-term evaluation of sensory function and useful for advancing somatosensory research [26]. In response, we hypothesized that QST for thermal thresholds may be useful for evaluating the sensory symptoms of PD. Patients with PD (in comparison to normal subjects) have been reported to show sensory impairment, with increased sensory thresholds for vibration [15] and increased 2-point discrimination thresholds in proprioception [17]. In a more recent study, PD patients showed sensory disturbances with decreased pain thresholds for cold and heat [3]. Thus, our CST and WST findings (Fig. 2) are consistent with previously reported studies demonstrating increased temperature sensory thresholds in PD patients [12].

The physiological mechanisms by which STN-DBS might improve temperature sensations in PD patients remains unclear; however, several hypotheses have been reported. Firstly, STN stimulation may lead indirectly to the activation of the somatosensory cortex and thereby lead to improved temperature sensation. In a previous FDG-PET study of bilateral STN-DBS, it was shown that during the DBS-on state, the regional cerebral metabolic rate of glucose consumption increased significantly in the midbrain, basal

**Table 2**
Sensory threshold in patients and control subjects.

| | CSTs | WSTs | CPTs | HPTs | CSTs | WSTs | CPTs | HPTs |
|---|---|---|---|---|---|---|---|---|
| Control subjects | 30.9 ± 0.2 | 33.9 ± 0.3 | 16.0 ± 2.3 | 43.0 ± 1.9 | | | | |
| | | More affected side | | | Less affected side | | | |
| PD patients in DBS-on | 29.0 ± 0.6 | 34.5 ± 0.3 | 17.7 ± 1.5 | 44.0 ± 0.9 | 29.7 ± 0.3 | 34.5 ± 0.3 | 21.1 ± 1.8 | 42.5 ± 1.1 |
| PD patients in DBS-off | 25.6 ± 1.0 | 36.7 ± 0.8 | 16.2 ± 2.0 | 45.0 ± 1.1 | 27.5 ± 0.8 | 36.2 ± 0.6 | 18.7 ± 2.1 | 43.2 ± 1.2 |
| *P* value[a] | NS | NS | NS | NS | NS | NS | NS | NS |
| *P* value[b] | <.001*** | .002** | NS | NS | .010* | .013* | NS | NS |

*P* > .05 by Dunnett multiple comparisons test. CST, cold sense threshold; WST, warm sense threshold; CPT, cold pain threshold; HPT, heat pain threshold; PD, Parkinson's disease; DBS-on, deep brain stimulation on; DBS-off, deep brain stimulation off; NS, not significant.

[a] Comparison between PD patients in the DBS-on mode and healthy control subjects.

[b] Comparison between PD patients in the DBS-off mode and healthy control subjects.

* *P* < .05.

** *P* < .01.

*** *P* < .001.

**Table 3**
Sensory thresholds in patients with PD.

| | CSTs | WSTs | CPTs | HPTs |
|---|---|---|---|---|
| Control subjects | 30.9 ± 0.1 | 33.9 ± 0.1 | 16.0 ± 1.7 | 43.0 ± 1.1 |
| Control subjects (after the interval of 30 minutes) | 30.7 ± 0.1 | 34.0 ± 0.3 | 15.9 ± 2.2 | 42.8 ± 1.8 |
| *P* value | NS | NS | NS | NS |
| DBS-on (PD patients) | 29.4 ± 0.8 | 34.5 ± 0.7 | 19.4 ± 1.6 | 43.2 ± 1.0 |
| DBS-off (PD patients) | 26.6 ± 0.8 | 36.5 ± 0.7 | 17.4 ± 1.6 | 44.1 ± 1.0 |
| *P* value[a] | <.001*** | <.001*** | NS | NS |
| More affected side (PD patients) | 27.3 ± 0.8 | 35.6 ± 0.7 | 16.9 ± 1.6 | 44.5 ± 1.0 |
| Less affected side (PD patients) | 28.6 ± 0.8 | 35.4 ± 0.7 | 19.9 ± 1.6 | 42.8 ± 1.0 |
| *P* value[b] | .020* | NS | .011** | .016** |

NS = $P > .05$. CST, cold sense threshold; WST, warm sense threshold; CPT, cold pain threshold; HPT, heat pain threshold; PD, Parkinson's disease; DBS-on, deep brain stimulation on; DBS-off, deep brain stimulation off; NS, not significant.
[a] Comparison between PD in the DBS-on mode and PD in the DBS-off mode.
[b] Comparison between the less affected side and the more affected side in PD patients.
* $P < .05$.
** $P < .01$.
*** $P < .001$.

ganglia area, frontal cortex, temporal cortex, and parietal cortex [5,22]. It has been determined that the posterior parietal region received afferents from prefrontal regions, the sensory cortex, and multiple thalamic relay nuclei [19]. Thus, STN-DBS may activate not only the frontal but also the parietal cortex, and a contribution of STN to sensory function, as well as to its roles in associative, limbic, and basal ganglia circuits, has been confirmed [5]. This metabolic change may result in an altered temperature sensation that is associated with parietal and basal ganglia circuits. Secondly, STN-DBS might normalize brain network abnormalities related to temperature sensation and pain perception. PD reportedly involves a generalized dysfunction of the entire neuronal network, probably resulting from impaired basal ganglia function, although the precise mechanism is not well understood [17].

In this study, we have used the method of limits for performing QST. It has been reported that sensory thresholds are dependent on a subject's reaction time in the method of limits [18]. Thus we may need to take into account the result of biased reaction times as a result of possible motor impairment, especially when undertaking QST on the less affected side of PD patients, because this may introduce a delayed response when they click the response button with their opposite and more affected side hand. If this was to have a significant impact on the final results, we would expect lower thresholds for CSTs and WSTs of the less affected hand. Despite this

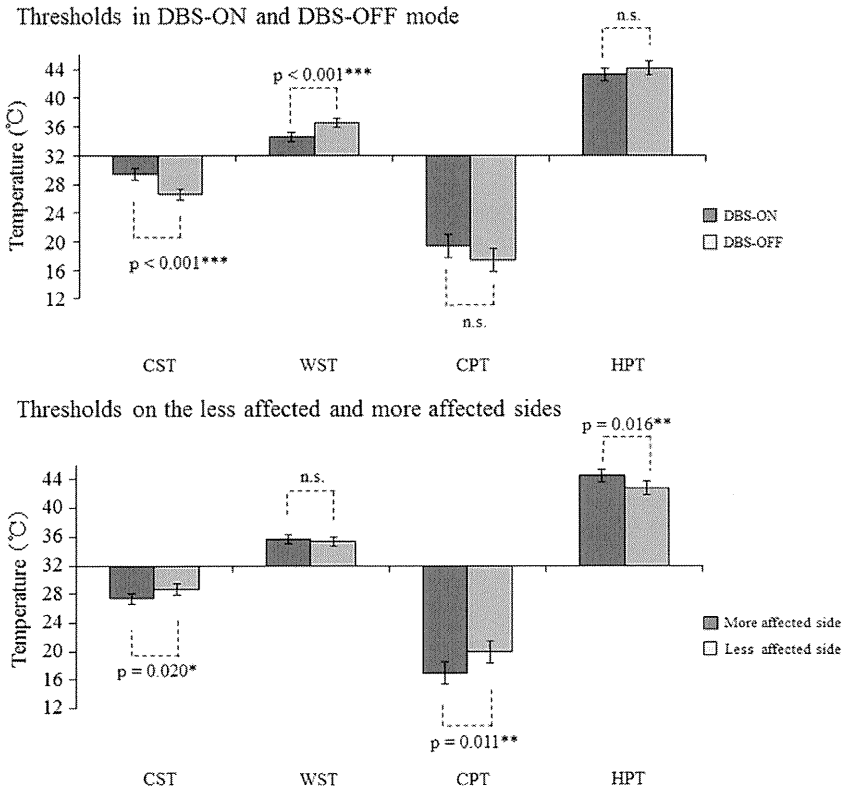


**Fig. 3.** Differences in sensory thresholds in patients with PD. CSTs and WSTs were significantly lower during the DBS-on state compared with the DBS-off state. CPTs and HPTs did not differ significantly between the DBS-on and DBS-off states. CPTs and HPTs were significantly lower on the less affected side than on the more affected side. A 2-factor repeated measures analysis of variance (ANOVA) was used to analyze differences. Error bars represent SEM. A *P* value of <.05 was considered statistically significant (*$P < .05$; **$P < .01$; ***$P < .001$; NS, $P > .05$). CPT, cold pain threshold; CST, cold sense threshold; DBS-on, deep brain stimulation on; DBS-off, deep brain stimulation off; HPT, heat pain threshold; PD, Parkinson's disease; WST, warm sense threshold.

possible bias, this was not the case. As was stated previously, the more affected hand was found to have lower thresholds for CSTs and WSTs. This would indicate that motor performance probably has little effect on the significance of the QST results in our study.

QST can be adversely affected by consecutive repeated tests. CSTs, WSTs, CPTs, and HPTs reportedly changed significantly with repeated testing [13]. Thus, researchers must be cautious when assessing the importance of changes in thermal sense thresholds. With this in mind, we performed a control experiment involving repeated QSTs with a 30-minute interval in between in 14 healthy control subjects. As a result, we found no significant differences between these 2 sessions separated by the interval of 30 minutes (Table 3). This result indicates that the sensory thresholds, CSTs and WSTs in particular, are probably not affected by repetitive QSTs separated by an interval of 30 minutes.

Only a few studies have addressed the effects of levodopa and dopamine agonists on sensory disorders in PD patients. Levodopa significantly reduced pain-induced activation in the posterior insula and anterior cingulate cortex in PD patients [1]. Our study did not include a baseline condition in which patients were completely free of antiparkinsonian medication. Indeed, the effect of levodopa on temperature sense thresholds may have influenced our results. However, it was not ethically possible for us to withdraw these medications from participating patients. It should, however, be noted that we consider the effects of drugs on our final results in this study to be minimized because DBS-on and DBS-off state temperature sensory thresholds and pain thresholds were compared in the same patients with all QST measurements being conducted within 1 hour of each other.

Our findings provide new insights into the mechanisms by which DBS improves sensory impairments, that is, via modulation of the disease-related brain network abnormality. Our findings suggest that STN-DBS can be used to modulate sensory pathways and improve temperature sensations in PD patients. Studies involving larger groups of patients are needed to show whether our findings reflect a general principle underlying the effect of STN-DBS on sensory information processing.

## Acknowledgements

This study was supported in part by the Grant-in-Aid for Scientific Research from the Japanese Ministry of Health, Labour and Welfare. There are no conflicts of interest.

## References

[1] Brefel-Courbon C, Payoux P, Thalamas C, Ory F, Quelven I, Chollet F, Montastruc JL, Rascol O. Effect of levodopa on pain threshold in Parkinson's disease: a clinical and positron emission tomography study. Mov Disord 2005;20:1557–63.

[2] Deuschl G, Schade-Brittinger C, Krack P, Volkmann J, Schafer H, Botzel K, Daniels C, Deutschlander A, Dillmann U, Eisner W, Gruber D, Hamel W, Herzog J, Hilker R, Klebe S, Kloss M, Koy J, Krause M, Kupsch A, Lorenz D, Lorenzl S, Mehdorn HM, Moringlane JR, Oertel W, Pinsker MO, Reichmann H, Reuss A, Schneider GH, Schnitzler A, Steude U, Sturm V, Timmermann L, Tronnier V, Trottenberg T, Wojtecki L, Wolf E, Poewe W, Voges J. A randomized trial of deep-brain stimulation for Parkinson's disease. N Engl J Med 2006;355:896–908.

[3] Djaldetti R, Shifrin A, Rogowski Z, Sprecher E, Melamed E, Yarnitsky D. Quantitative measurement of pain sensation in patients with Parkinson disease. Neurology 2004;62:2171–5.

[4] Hagander LG, Midani HA, Kuskowski MA, Parry GJ. Quantitative sensory testing: effect of site and skin temperature on thermal thresholds. Clin Neurophysiol 2000;111:17–22.

[5] Hilker R, Voges J, Weisenbach S, Kalbe E, Burghaus L, Ghaemi M, Lehrke R, Koulousakis A, Herholz K, Sturm V, Heiss WD. Subthalamic nucleus stimulation restores glucose metabolism in associative and limbic cortices and in cerebellum: evidence from a FDG-PET study in advanced Parkinson's disease. J Cereb Blood Flow Metab 2004;24:7–16.

[6] Jaaskelainen SK, Teerijoki-Oksa T, Forssell H. Neurophysiologic and quantitative sensory testing in the diagnosis of trigeminal neuropathy and neuropathic pain. Pain 2005;117:349–57.

[7] Jobst EE, Melnick ME, Byl NN, Dowling GA, Aminoff MJ. Sensory perception in Parkinson disease. Arch Neurol 1997;54:450–4.

[8] Kaji R, Urushihara R, Murase N, Shimazu H, Goto S. Abnormal sensory gating in basal ganglia disorders. J Neurol 2005;252:IV13–6.

[9] Kumar R, Lozano AM, Kim YJ, Hutchison WD, Sime E, Halket E, Lang AE. Double-blind evaluation of subthalamic nucleus deep brain stimulation in advanced Parkinson's disease. Neurology 1998;51:850–65.

[10] Limousin P, Krack P, Pollak P, Benazzouz A, Ardouin C, Hoffmann D, Benabid AL. Electrical stimulation of the subthalamic nucleus in advanced Parkinson's disease. N Engl J Med 1998;339:1105–11.

[11] Lozano AM, Dostrovsky J, Chen R, Ashby P. Deep brain stimulation for Parkinson's disease: disrupting the disruption. Lancet Neurol 2002;1:225–31.

[12] Nolano M, Provitera V, Estraneo A, Selim MM, Caporaso G, Stancanelli A, Saltalamacchia AM, Lanzillo B, Santoro L. Sensory deficit in Parkinson's disease: evidence of a cutaneous denervation. Brain 2008;131:1903–11.

[13] Palmer ST, Martin DJ. Thermal perception thresholds recorded using method of limits change over brief time intervals. Somatosens Mot Res 2005;22:327–34.

[14] Palmer ST, Martin DJ, Steedman WM, Ravey J. Effects of electric stimulation on C and A delta fiber-mediated thermal perception thresholds. Arch Phys Med Rehabil 2004;85:119–28.

[15] Pratorius B, Kimmeskamp S, Milani TL. The sensitivity of the sole of the foot in patients with Morbus Parkinson. Neurosci Lett 2003;346:173–6.

[16] Sandyk R, Snider SR. Sensory symptoms: Parkinson's disease. Neurology 1985;35:619–20.

[17] Schneider JS, Diamond SG, Markham CH. Parkinson's disease: sensory and motor problems in arms and hands. Neurology 1987;37:951–6.

[18] Shy ME, Frohman EM, So YT, Arezzo JC, Cornblath DR, Giuliani MJ, Kincaid JC, Ochoa JL, Parry GJ, Weimer LH. Quantitative sensory testing: report of the therapeutics and technology assessment subcommittee of the American academy of neurology. Neurology 2003;60:898–904.

[19] Taktakishvili O, Sivan-Loukianova E, Kultas-Ilinsky K, Ilinsky IA. Posterior parietal cortex projections to the ventral lateral and some association thalamic nuclei in Macaca mulatta. Brain Res Bull 2002;59:135–50.

[20] Tinazzi M, Recchia S, Simonetto S, Tamburin S, Defazio G, Fiaschi A, Moretto G, Valeriani M. Muscular pain in Parkinson's disease and nociceptive processing assessed with $CO_2$ laser-evoked potentials. Mov Disord 2010;25:213–20.

[21] Tinazzi M, Del Vesco C, Fincati E, Ottaviani S, Smania N, Moretto G, Fiaschi A, Martino D, Defazio G. Pain and motor complications in Parkinson's disease. J Neurol Neurosurg Psychiatry 2006;77:822–5.

[22] Trost M, Su S, Su P, Yen RF, Tseng HM, Barnes A, Ma Y, Eidelberg D. Network modulation by the subthalamic nucleus in the treatment of Parkinson's disease. Neuroimage 2006;31:301–7.

[23] Verdugo R, Ochoa JL. Quantitative somatosensory thermotest. A key method for functional evaluation of small calibre afferent channels. Brain 1992;115:893–913.

[24] Yarnitsky D. Quantitative sensory testing. Muscle Nerve 1997;20:198–204.

[25] Yarnitsky D, Ochoa JL. Studies of heat pain sensation in man: perception thresholds, rate of stimulus rise and reaction time. Pain 1990;40:85–91.

[26] Zaslansky R, Yarnitsky D. Clinical applications of quantitative sensory testing (QST). J Neurol Sci 1998;153:215–38.

ORIGINAL ARTICLE

# Electrocorticographic Control of a Prosthetic Arm in Paralyzed Patients

Takufumi Yanagisawa, MD, PhD,[1,2] Masayuki Hirata, MD, PhD,[1] Youichi Saitoh, MD, PhD,[1,5] Haruhiko Kishima, MD, PhD,[1] Kojiro Matsushita, PhD,[1] Tetsu Goto, MD, PhD,[1] Ryohei Fukuma, MS,[2,3] Hiroshi Yokoi, PhD,[4] Yukiyasu Kamitani, PhD,[2,3] and Toshiki Yoshimine, MD, PhD[1]

**Objective:** Paralyzed patients may benefit from restoration of movement afforded by prosthetics controlled by electrocorticography (ECoG). Although ECoG shows promising results in human volunteers, it is unclear whether ECoG signals recorded from chronically paralyzed patients provide sufficient motor information, and if they do, whether they can be applied to control a prosthetic.

**Methods:** We recorded ECoG signals from sensorimotor cortices of 12 patients while they executed or attempted to execute 3 to 5 simple hand and elbow movements. Sensorimotor function was severely impaired in 3 patients due to peripheral nervous system lesion or amputation, moderately impaired due to central nervous system lesions sparing the cortex in 4 patients, and normal in 5 patients. Time frequency and decoding analyses were performed with the patients' ECoG signals.

**Results:** In all patients, the high gamma power (80–150Hz) of the ECoG signals during movements was clearly responsive to movement types and provided the best information for classifying different movement types. The classification performance was significantly better than chance in all patients, although differences between ECoG power modulations during different movement types were significantly less in patients with severely impaired motor function. In the impaired patients, cortical representations tended to overlap each other. Finally, using the classification method in real time, a moderately impaired patient and 3 nonparalyzed patients successfully controlled a prosthetic arm.

**Interpretation:** ECoG signals appear useful for prosthetic arm control and may provide clinically feasible motor restoration for patients with paralysis but no injury of the sensorimotor cortex.

ANN NEUROL 2012;71:353–361

Paralyzed patients and amputees would benefit from cortically controlled prosthetics in the form of a brain–computer interface (BCI). Among the possible cortical signals available for BCI, electrocorticography (ECoG) offers one of the most clinically feasible options, having superior long-term stability and lower technical difficulty compared with other invasive signals.[1,2] Evidence from studies with nonparetic patients with epilepsy shows that some movements or movement intentions can be inferred from ECoG signals accurately enough to control external devices such as a computer cursor.[3–6] However, it is unclear whether these findings are applicable to paralyzed patients, whose sensorimotor cortices may have undergone extensive reorganization after deefferentation and deafferentation of the paralyzed body parts.

Paresis-associated cortical reorganization may modify ECoG signals of the sensorimotor cortex. Cortical reorganization occurs in the sensorimotor cortex of individuals with spinal cord injuries,[7–9] limb amputations,[10–12] and stroke.[13–15] Such cortical reorganizations have been shown to alter functional activations in the

View this article online at wileyonlinelibrary.com. DOI: 10.1002/ana.22613

Received Feb 4, 2011, and in revised form Aug 4, 2011. Accepted for publication Aug 12, 2011.

Address correspondence to Dr Hirata, Department of Neurosurgery, Osaka University Medical School, E6 2-2 Yamadaoka Suita, Osaka, Japan. E-mail: mhirata@nsurg.med.osaka-u.ac.jp or Dr Kamitani, ATR Computational Neuroscience Laboratories, 2-2-2 Hikaridai, Seika, Soraku, Kyoto 619-0288, Japan. E-mail: kmtn@atr.jp

[1]Department of Neurosurgery, Osaka University Medical School, Osaka; [2]ATR Computational Neuroscience Laboratories, Kyoto; [3]Nara Institute of Science and Technology, Nara; and [4]University of Tokyo Interfaculty Initiative in Information Studies Graduate School of Interdisciplinary Information Studies, Tokyo, Japan; [5]Department of Neuromodulation and Neurosurgery office for University-Industry Collaboration, Osaka, Japan.

Additional supporting information can be found in the online version of this article.

 

TABLE 1: Clinical Profiles

| Patient No. | Age, yr/Sex | Diagnosis | Duration of Disease, yr | Paresis in Affected Limb (MMT) | Sensation in Affected Limb |
|---|---|---|---|---|---|
| N1 | 34/F | R intractable epilepsy | 19 | None | Normal |
| N2 | 14/M | R intractable epilepsy | 7 | None | Normal |
| N3 | 20/F | L intractable epilepsy | 6 | None | Normal |
| N4 | 22/F | R intractable epilepsy | 10 | None | Normal |
| N5 | 13/M | L intractable epilepsy | 11 | None | Normal |
| P1 | 49/M | R putaminal hemorrhage | 2 | Slightly spastic (5−) | Hypoesthesia |
| P2 | 66/F | R subcortical infarction | 3.3 | Spastic (4) | Hypoesthesia |
| P3 | 64/M | R thalamic hemorrhage | 7 | Spastic (4) | Hypoesthesia |
| P4 | 65/M | Ruptured spinal dAVF | 8 | Spastic (4) | Hypoesthesia |
| S1 | 31/M | L brachial plexus avulsion | 5 | Complete (0)[a] | Anesthesia |
| S2 | 49/M | L brachial plexus avulsion | 6 | Severe (1)[a] | Severe hypoesthesia |
| S3 | 47/M | Amputation below L shoulder | 3.3 | No arm | None |

[a]Post transplantation of intercostal nerve.
dAVF = dural arteriovenous fistula; F = female; L = left; M = male; MMT = manual muscle test; R = right.

cortices and affect motor function,[14] sensation, and recognition of body parts.[10,11,16] However, quantitative data are lacking on altered functional activations of the sensorimotor cortex after cortical reorganization and subsequent modification of ECoG signals.

We examined ECoG signals of nonparalyzed patients and patients with different levels of motor dysfunctions to quantitatively address 3 questions: (1) Do the ECoG signals of patients with chronic motor dysfunctions show preservation of spatiotemporal patterns of activation even after reorganization? (2) How much are ECoG activation maps for different motor tasks modified in the reorganized sensorimotor cortex? and (3) Can ECoG activation be applicable to controlling a prosthetic arm?

## Patients and Methods

### *Patient Population*

Twelve patients (4 female, 8 male; age range, 13–66 years) with subdural electrodes participated in this study. The patients had different degrees of motor dysfunctions and sensory disturbances (Table 1). Five patients (N1–N5) with epilepsy had no motor dysfunctions; 4 patients (P1–P4) had spastic paresis and weakness in their upper limbs due to strokes without damage to the sensorimotor cortex (moderate motor dysfunction); and 3 patients (S1–S3) had severely impaired sensorimotor function of their limbs due to brachial plexus root avulsion or amputation (severe motor dysfunction; Supplementary Methods). Patients S1–S3 differed in their ability to imagine movement of their affected limbs (Table 2). All participants or their guardians gave written informed consent to participate in the study, which was approved by the ethics committee of Osaka University Hospital.

All patients had been implanted with subdural electrode arrays that covered a broad sensorimotor cortical area, including the hand motor strip. These arrays were kept in place for 2 weeks to determine either the epileptic foci or the optimal stimulation sites to achieve maximum pain reduction.[17] At the end of these 2 weeks, the arrays were removed. In impaired patients, 4 permanent electrodes were then placed at the sites where stimulation provided optimal pain control.

### *Movement Tasks*

Experiments were performed in an electromagnetically shielded room approximately 1 week after electrode placement. The first session was designed to train the decoder on the ECoG signals (decoder training session). Patients performed 1 of 3 possible movement tasks that differed by the set of movement types that were executed: (1) grasping, thumb flexion, and elbow flexion (P1, P2, S1–S3); (2) grasping, pinching, hand-opening, elbow flexion, and tongue protrusion (P3); or (3) grasping, pinching, hand-opening, elbow flexion, and elbow extension (N1–N5, P4). For movement task 3, the patients were first instructed to perform the 3 hand movements. Then, after a free-run session in which patients undertook movements at their own pace, if they were able to undertake additional sessions without fatigue, they were instructed to perform 5 movements, preferably ones involving the elbow. Grasping and elbow flexion were commonly performed among all patients, although we selected the

TABLE 2: Summary of the Decoding Results

| Patient No. | Ability to Imagine Movements | % Correct (grasp vs elbow) | Mean ± SD | % Correct (move vs rest) | Mean ± SD |
|---|---|---|---|---|---|
| N1 | | 92.9 | 92.5 ± 3.4 ($p < 0.05$) | 96.6 | 93.6 ± 4.4 (NS) |
| N2 | | 98.2 | | 94.5 | |
| N3 | | 90.7 | | 86.0 | |
| N4 | | 90.5 | | 94.2 | |
| N5 | | 90.0 | | 96.4 | |
| P1 | | 86.7 | 89.2 ± 5.8 (NS) | 95.7 | 95.6 ± 4.5 (NS) |
| P2 | | 85.7 | | 100.0 | |
| P3 | | 97.9 | | 89.5 | |
| P4 | | 86.7 | | 97.3 | |
| S1 | Easy | 90.3 | 71.3 ± 17.0 ($p < 0.05$) | 98.2 | 93.2 ± 4.6 (NS) |
| S2 | Slightly difficult | 57.3 | | 92.2 | |
| S3 | Difficult | 66.3 | | 89.2 | |

NS = not significant; SD = standard deviation.

3 types of movement tasks to adjust the way patients could control the prosthesis.

The patients selected and performed one of the movements within a presented task after being cued with auditory beeps (Fig 1A). The patients were instructed to execute movements immediately after the third beep and then return their hands or elbows to a resting position. For the resting position, patients were instructed to relax their hands or elbows with slightly flexed joints. Each type of movement was performed approximately 30 to 100 times. Patients S1–S3 were instructed to attempt the movements of their affected limbs immediately after the auditory cue. The movement instructions were delivered using a PC monitor controlled by ViSaGe (Cambridge Research System, Rochester, UK) placed in front of the patients. The decoder training session was open loop. The patients were not informed of the classifier results and therefore did not have an opportunity for learning or improving their performance.

After the decoder training session, 4 patients repeated the same task they had performed during the session, but at self-paced intervals without external cues (free-run session, see Fig 1B). These patients had recently performed the task and were able to continue without extensive fatigue. Without receiving further training, they were instructed to control the prosthetic arm by performing their hand and elbow movements. Patient N1 could not control the elbow of the prosthetic arm due to mechanical problems of the prosthesis.

## ECoG Recording and Preprocessing

For each patient, 15 to 60 planar-surface platinum grid electrodes were placed over the sensorimotor cortex and within the central sulcus (intrasulcal electrodes)[18] (see Supplementary Methods). Video recording and electromyographic (EMG electrode; Nihon Koden, Tokyo, Japan) recordings of their hands and arms were performed solely to identify the performed movements.

ECoGs were recorded and digitized at a sampling rate of 1,000Hz. During the decoder training session, the ECoG signals were obtained time-locked to the cue signal. In the free-run session, 1-second duration ECoG signals were recorded online at 200-millisecond intervals. A fast Fourier transformation (FFT; EEGLAB v5.03) was performed for each 1-second signal to obtain the power of each of the 3 frequency bands (2–8, 8–25, and 80–150Hz) for each electrode. We used FFT to complete the online decoding over the 200 milliseconds. The 3 frequency bands were chosen based on our previous studies.[19]

## Decoding Algorithms and Prosthetic Hand Control

To infer, or decode, the movement types executed or attempted by the patients, we constructed a linear classifier trained by a linear support vector machine, the SVM decoder (see Supplementary Methods).[18,20,21] The trained SVM decoder was inputted with the ECoG signals to output an inferred movement type. A 5-fold cross-validation was used to test how well the decoder could generalize.

To apply the SVM decoder to the free-run sessions without external cues, we developed another decoder (GPR decoder; see Supplementary Methods). The trained GPR decoder was also inputted with the ECoG signals to output an estimated